Available online at www.sciencedirect.com
SCIENCE DIRECT®
Earth and Planetary Science Letters 222 (2004) 751–765
EPSL
www.elsevier.com/locate/epsl

Contributions of an ancient evaporitic-type reservoir to subglacial Lake Vostok chemistry

M. De Angelis[a,*], J.-R. Petit[a], J. Savarino[a], R. Souchez[b], M.H. Thiemens[c]

[a] LGGE CNRS/UJF BP 96, 38402 Saint Martin d'Hères, France
[b] Département des Sciences de la Terre, Université Libre de Bruxelles, 50 Av. F.D. Roosevelt, B-1050 Brussels, Belgium
[c] Department of Chemistry and Biochemistry, University of California, San Diego, La Jolla, CA 92093-0356, USA

Received 25 July 2003; received in revised form 15 March 2004; accepted 17 March 2004

Abstract

We present here the first comprehensive study of the chemical composition of accretion ice from Lake Vostok. Ion chromatographic analyses were performed on samples obtained along the deeper part of the Vostok ice core. Samples were taken from 3350 down to 3611 m depth, both in glacier ice and subglacial lake ice. The total ionic contents of two accretion ice layers—a few meters thick and centered around 3540 and 3590 m depth—are several times lower than those of glacier ice. Very low concentrations were also observed in the deeper part of accretion ice, below 3609 m depth. Elsewhere, the total ionic content is variable but remains 5 to 50 times higher than in glacier ice. Whatever its total ionic content, the ionic composition of accretion ice is significantly different from what is observed in glacier ice. It is dominated by sodium chloride, homogeneously distributed throughout the ice lattice, as well as calcium and magnesium sulfate, likely located in solid inclusions, or to a lesser extent at grain boundaries. Chemical considerations combined with additional studies of sulfur and oxygen isotopes in sulfate, and iron measurements strongly suggest that glacier water recycling and bedrock hydrolysis do not play a prominent role in providing impurities to accretion ice. It is more likely that NaCl rich water carrying fine sulfate salt particles is sporadically incorporated in the ice accreting in a shallow bay upstream from Vostok. The origin of such salty water, which should also contribute to Lake salinity, is discussed.

Keywords: Antarctica; Lake Vostok; accretion ice; ice composition

1. Introduction

The largest subglacial lake identified under the Antarctic ice cap is Lake Vostok [1,2]. The lake is 230 km long and 50 km wide. The water depth varies with ice thickness and reaches 600 m in its southern part below the drilling site where the ice is 3750 m thick. The configuration of the ice, the underlying lake and the bedrock, along with main glacier flow pattern, is shown schematically in Fig. 1.

Evidence from water isotope studies and ice properties such as crystal sizes, electrical conductivity and total gas content show that the deeper part of the Vostok ice core is made of two distinct types of ice separated by a sharp transition. Above 3538 m depth, the ice is meteoric, originating from the ice sheet,

* Corresponding author. Tel.: +33-4-76-82-42-33; fax: +33-4-76-82-42-01.
E-mail address: ange@lgge.obs.ujf-grenoble.fr (M. De Angelis).

0012-821X/$ - see front matter © 2004 Elsevier B.V. All rights reserved.
doi:10.1016/j.epsl.2004.03.023

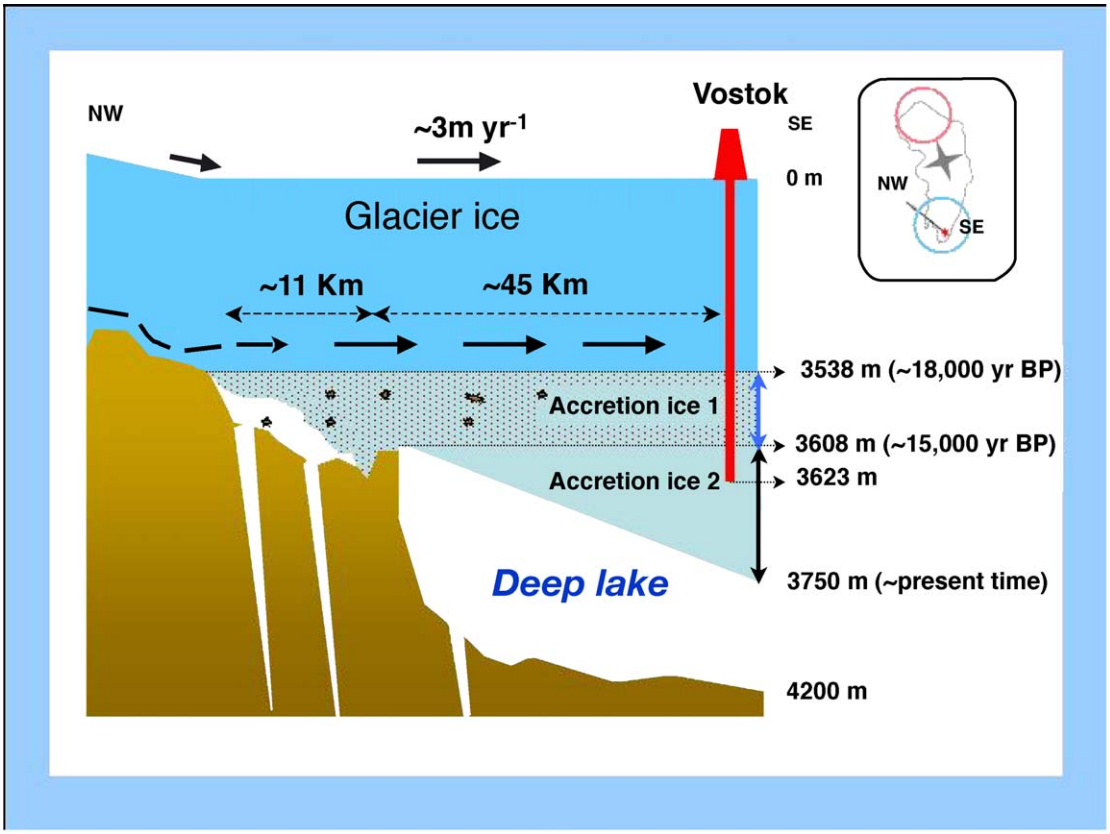

Fig. 1. Cross-section of the ice sheet and the lake along the flow line passing by Vostok. The ice sheet flows from NW to SE. The glacier comes afloat in the lake in a shallow bay and then passes over a bedrock rise 11 km from the shore. The bank is steep and the glacier tongue floats over the deep main lake. Vostok is located ~ 56 km from the head of the shallow bay. The mean ice velocity of the glacier tongue (~ 3 m year^{-1}) can be used to estimate transit times and mean accretion rates. The two main layers of accretion ice (see text) are shown: accretion ice-1 contains visible inclusions while accretion ice-2 appears to be clean. In the inset, melting and accretion zones are roughly represented by red and blue circles, respectively.

while below 3539 m it originates from accretion, i.e. refreezing of the lake water [3]. The ice thickness above the lake varies from 3750 m in its southern part to 4150 m in its northern part so that the ice ceiling is tilted. Based on radio-echo soundings, subglacial melting occurs at the ice–lake interface in the northern part of the lake while accretion takes place below Vostok station, in the southern part of the lake [4,5]. The isotopic composition of the accretion ice supports the hypothesis that lake ice forms by freezing and consolidation of a slush made of frazil ice and host water, and clearly indicates that the lake does not contain sea water [6]. It also suggests that the lake is not a closed water reservoir. However, very few data are available regarding its chemistry, which would provide valuable information concerning the formation and dynamics of the lake.

Two main types of accreted ice may be distinguished (Fig. 1): in the upper part, the ice (accretion ice-1) contains many visible inclusions, mainly located between 3540 and 3608 m depth [3]. These inclusions vanish when samples are melted, and their composition remains unknown. However, preliminary studies of their insoluble part have been carried out by optical microscopy and show that some contain fine particles (clays or quartz, and dust of unidentified origin). Below 3608 m, the ice is clear, without visible inclusions (accretion ice-2).

Although not represented in Fig. 1, two other thin layers of ice containing no or very few visible

inclusions (ice-2 type) are observed: the first is located just below the glacier ice (3538–3553) and the second from 3588 to 3594 m depth. Based on topography data from radio-echo-sounding studies [7] and flow trajectory calculation, the first 60 m of accretion ice (accretion ice-1) were likely formed in a shallow bay located northeast of the drilling site and partly separated from the deeper main lake by a submerged reef (see Fig. 1), while deeper on (below 3608 m), the ice (accretion ice-2) originates from the main lake. Taking into account the ice flow velocity (3 m $year^{-1}$) and trajectory, apparent accretion rates varying from 3.8 cm $year^{-1}$ over the shallow bay to 1.4–2.5 cm $year^{-1}$ over the main lake may be calculated.

This paper presents the chemical composition of glacier and accretion ice and discusses the possible composition of lake water and origin of sub-glacial deposits. The interpretation of this first set of data is supported by additional measurements of sulfate isotopic composition and total iron in a few selected samples.

2. Methods and sampling

Ice cross-sections, a few centimeters thick and roughly 10 cm long, were cut from the inner part of available core pieces with a band saw. They were cleaned in three successive baths of ultra-pure water until roughly half the initial ice volume was removed. Despite the small initial size of these ice cross-sections and strong core contamination by drilling fluid, the concentrations of trace species that are very sensitive to contamination, such as K^+, NH_4^+ and carboxylic ions ($HCOO^-$ or CH_3COO^-), are very similar to those obtained from another east Antarctic ice core extracted without drilling fluid [8]. This demonstrates the effectiveness of the present cleaning procedure. Once decontaminated, ice samples were put in air-tight glass bottles and kept frozen until analysis.

Major mineral ions and four organic ions (Na^+, NH_4^+, K^+, Mg^{2+}, Ca^{2+}, F^-, $HCOO^-$, CH_3COO^-, $CH_3SO_3^-$, Cl^-, NO_3^-, SO_4^{2-}, $C_2O_4^{2-}$) were determined by ion chromatography. Typical detection limits corresponding to injection loop volumes of 1.5 ml were lower than 0.1 ng g^{-1} for Na^+, NH_4^+, K^+, Mg^+, F^- and NO_3^-, and in the range of 0.5 ng g^{-1} for the other ions. Analytical uncertainties ranged from 3% to 5% depending on concentration range. An attempt to determine NO_2^- was made but concentrations remained below the detection limit (0.5 ng g^{-1}).

For isotopic analysis, ~ 300 ml of decontaminated accreted ice were reduced to approximately 30 ml by gentle, non-boiling heated evaporation. The sulfate was collected on a concentration ion exchange column and separated from all other species in the sample. The separated sulfate was finally analyzed for oxygen and sulfur isotope composition by mass spectrometry using a newly developed pyrolysis technique [9]. The procedure involves first converting the purified soluble sulfate to Ag_2SO_4 using an ion exchange membrane. The Ag_2SO_4 sample is then freeze-dried in a quartz boat and pyrolysed to O_2, SO_2, and Ag metal in a continuous flow system. O_2 is isolated and then measured on a Finnigan MAT 251 IRMS. Based on replica standard and sample measurements, $\delta^{18}O$, $\delta^{17}O$ and $\Delta^{17}O$ uncertainties are estimated to be ± 0.5‰, ± 0.3‰ and ± 0.1‰ (1σ), respectively [9]. The isolated SO_2 is used for sulfur isotope analysis. Sulfur dioxide is transferred to a sample tube filled with 30% H_2O_2 solution. After conversion to sulfuric acid, excess $BaCl_2$ is added to the solution and a $BaSO_4$ precipitate forms. The solution is then evaporated to dryness. The next steps, including extraction, purification, concentration and conversion of sulfate to SF_6 for IRMS analysis use well-established analytical procedures [10–12]. Sulfur isotope ratios are expressed in delta notation with respect to the Canyon Diablo Triolite (CTD). Uncertainties for $\delta^{34}S$, $\delta^{33}S$, $\Delta^{33}S$ are better than ± 0.05‰, 0.1‰, and 0.1‰, respectively.

3. Results

3.1. Concentration trends

From 3350 m down to 3535 m, samples were taken every 3 m and none of the ionic species studied displays an observable trend. Mean values calculated on this core section are presented in Table 1 along with concentration ranges corresponding to typical interglacial and full glacial climate conditions. Although stratigraphic perturbations have been observed in this part of the core [9,13], concentrations show

Table 1
Comparison between concentrations measured along the deeper part of glacier ice and typical concentration ranges during Holocene and LGM time periods

	F^-	MSA	Cl^-	NO_3^-	SO_4^{2-}	Na^+	NH_4^+	K^+	Mg^{2+}	Ca^{2+}
	(Concentrations are in ng g^{-1})									
Glacier ice (3350–3535 m) N = 60										
Mean	0.29	25	65	25	144	40	1.41	1.22	7.3	10.1
Standard deviation	0.21	6.3	21	11	32	8.0	0.31	0.40	2.9	5.9
Holocene										
Range	0.1–0.2	1.5–7.0	10–14	11–23	90–150	20–30	0.5–0.7	1.1–2.5	2.5–4.5	0.5–2.5
Last glacial maximum										
Range	0.7–1.6	13–36	78–250	50–130	170–300	80–160	1.0–2.0	5–15	15–30	18–84

very low variations (less than 50% of mean values). Minima are a few times higher than typical interglacial values and maxima significantly lower than those observed in ice formed under full glacial conditions. This suggests that at this depth, ice originates from the ice sheet but was formed under mild glacial conditions.

Below 3535 m, drastic changes can be observed in most of concentration profiles. Three distinctive trends, represented by the magnesium, methanesulfonate (MSA) and formate depth profiles in Fig. 2a, b and c, respectively, are observed when passing from glacier to accreted ice: Fig. 2a) the concentration profiles of several species (F^-, Cl^-, SO_4^{2-}, Na^+, Mg^{2+}, Ca^{2+}) strongly increase, attaining values sometimes more than one order of magnitude higher than in glacier ice samples corresponding to glacial maxima, Fig. 2b) MSA and NO_3^- concentrations sharply decrease in accreted ice where MSA becomes lower than the detection limit. The oxidized nitrogen ($NO_3^- + NO_2^-$) concentration at 3603 m (0.5 ng g^{-1}) is lower by more than one order of magnitude than data previously published by Karl et al. (~ 10 ng g^{-1}) [14], Fig. 2c) concentrations of a few species (NH_4^+ and carboxylate) remain relatively unchanged. The relative contribution of carbon from carboxylic acids remains close to zero regardless of the type of ice, suggesting an organic-carbon content lower than a few ng g^{-1} in accreted ice as well as in glacier ice, which is in agreement with preliminary DOC measurements in the range of a few ng g^{-1} (M. Shock, personal communication).

Detailed data are presented in Table 2. Depth profiles of sulfate, chloride, ammonium and nitrate are reported in Fig. 3, along with the number of visible inclusions and the ionic budget. The three layers of ice containing no visible inclusion (accretion ice-2), represented by shadowed areas in Table 2 and gray arrows in Fig. 3, correspond to concentration minima of all ions. Ion concentrations, even remaining very low (NH_4^+) or sharply decreasing (NO_3^-) at the glacier-accretion ice transition, are lower by one order of magnitude in accretion ice-2 than elsewhere in inclusion rich accretion ice (accretion ice-1). Only fluoride shows a less marked change (factor of 2 as a mean), probably due to its higher diffusion coefficient in ice (discussed in Section 4.1). Contrary to what was observed in glacier ice, some ions, such as SO_4^{2-}, exhibit very scattered concentration profiles in accretion ice-1, with peaks 10 times higher than background concentrations (see also Table 2). Other ions, like Cl^- or NO_3^-, do not vary as much, with a maximum to background concentration ratio close to 2 or lower. Lastly, no direct relationship can be inferred between any specific ion and the number of visible inclusions, which decreases with increasing depth and exhibits 5 broad relative maxima denoted A, B, C, D, and E apparently associated with varying ionic combinations.

3.2. Chemical composition

3.2.1. Relative ion contributions

SO_4^{2-} and Cl^- are the most abundant anionic species but a noticeable change in mean ionic mass distributions is observed when passing from glacier ice to accretion ice-1 and -2. The relative contribution of Cl^- progressively increases from 20% in

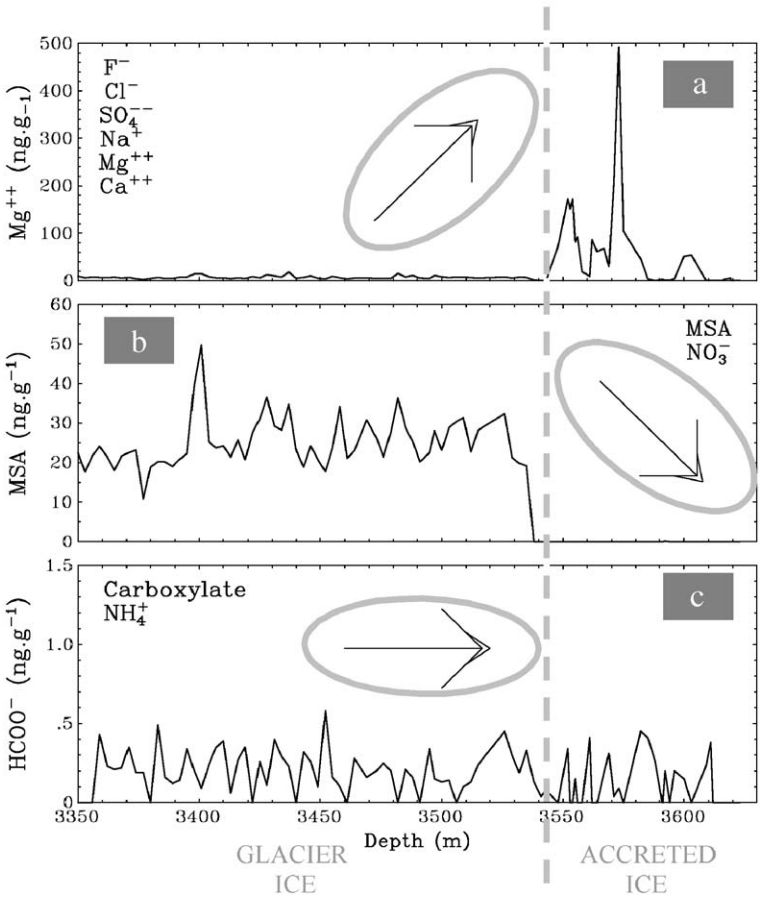

Fig. 2. Concentration as a function of depth. Concentrations are expressed in ng g^{-1}. Magnesium (Fig. 2a), MSA (Fig.2-b) and formate (Fig. 2-c) depth profiles are represented. Ions showing the same trend are listed in corresponding sub-figures.

glacier ice to 36% in accretion ice-1, and reaches 39% in the deeper layer of accretion ice-2, while the SO_4^{2-} contribution conversely decreases (46% and 36%, 20% of total ionic contents measured in glacier ice, accretion ice-1, and -2, respectively). A significant increase is also observed for sodium (13%, 20% and 25%, in glacier, accretion ice-1 and -2, respectively). The relative contribution of Ca^{2+} is significantly lower in glacier ice (3.0%) than in accretion ice-1 (5.6%) or -2 (8.0%). Mg^{2+} is also less abundant in glacier ice (2.2%) than in accretion ice-1 (3.7%) or -2 (3.0%). Significant contributions of other ions are observed only in glacier ice, where MSA amounts to ca 8% of total ionic content as does NO_3^-.

3.2.2. Ion associations

Ion associations in glacier and accreted ice are also different. As shown in Fig. 4a, Na^+ is tightly correlated ($r = 0.97$) to Cl^- in accretion ice-1 and -2 (stars). The regression slope is close to 1 (1.03 ± 0.06) and the intercept (0.44 ± 0.52 μEq l^{-1}) is low if compared to the Na^+ concentration range, which strongly suggests that these ions are present as NaCl. Due to fractionation processes affecting marine aerosol over Antarctica, Na^+ remains correlated ($r = 0.83$) to Cl^- in glacier ice (circles), but the regression slope is significantly lower (0.48 ± 0.04) than in accretion ice, and the intercept (0.85 ± 0.03 μEq l^{-1}) is close to the Na^+ concentration range (1–3 μEq l^{-1}). This difference between glacier ice and accretion ice is of importance

Table 2
Ionic composition of accreted ice

Depth	F^-	MSA	Cl^-	NO_3^-	SO_4^{2-}	Na^+	NH_4^+	K^+	Mg^{2+}	Ca^{2+}
Concentrations are in ng g^{-1}										
METEORIC ICE (3350 – 3535 m)										
Mean	0.29	25.0	65.2	25.3	144	40.2	1.41	1.2	7.3	10.1
σ	0.21	6.3	21.2	11.1	32	8.0	0.31	0.4	2.9	5.9
ACCRETED ICE –1 and –2										
3538	0.10	0.00	3.0	0.36	1.9	0.9	0.63	0.2	1.7	2.0
3541	0.92	0.00	5.9	0.76	34.7	5.7	0.07	0.6	0.4	15.2
3543	1.38	0.00	17.3	0.25	12.3	11.2	0.24	0.3	0.4	5.7
3548	3.42	0.00	516.3	1.46	519.2	275.1	1.32	5.8	71.5	27.2
3552	4.35	0.00	912.8	2.30	6223.6	539.0	1.73	9.4	172.0	1943.6
3553	2.85	0.00	1000.3	2.39	1145.7	752.6	3.7	7.4	151.8	202.7
3554	5.64	0.00	1147.8	2.74	2208.0	830.3	1.17	21.1	171.8	385.7
3555	2.61	0.00	686.1	1.78	624.9	366.3	2.3	6.4	81.4	38.5
3556	9.48	0.00	870.7	3.09	1236.6	620.6	1.7	7.9	92.8	386.3
3558	3.08	0.00	510.8	1.25	855.6	279.9	1.5	4.9	18.7	232.6
3561	5.24	0.00	804.0	1.55	146.2	402.3	1.43	5.5	9.3	34.6
3562	9.05	0.00	897.3	3.43	951.9	629.8	1.69	14.1	86.7	136.7
3564	2.98	0.00	565.3	1.54	786.6	318.2	1.18	10.3	61.6	120.1
3567	2.91	0.00	572.8	1.20	624.5	317.0	1.22	7.4	67.9	66.1
3569	3.33	0.00	625.3	2.17	305.4	330.8	2.25	10.0	30.0	38.7
3571	2.11	0.00	717.6	2.92	1355.2	598.9	2.42	8.5	207.4	201.3
3573	3.20	0.00	591.2	2.70	2995.7	447.3	1.34	15.1	491.9	178.2
3575	6.11	0.00	1233.2	2.06	535.8	921.2	1.16	11.7	104.3	46.2
3582	3.76	0.00	357.4	0.47	274.7	185.7	1.84	3.8	45.9	9.0
3585	2.31	0.00	225.5	0.59	62.6	128.6	1.45	4.0	3.8	13.0
3588	2.15	0.00	46.8	0.13	109.7	28.3	0.54	0.7	0.5	32.3
3591	1.16	0.00	22.9	0.08	20.1	17.6	0.06	0.2	3.2	5.9
3592	1.75	0.17	20.8	0.10	30.1	13.1	0.29	0.2	1.3	8.8
3594	1.62	0.00	17.6	0.12	0.7	10.1	0.65	0.3	1.1	4.3
3596	5.71	0.00	653.0	0.00	118.3	311.6	2.71	4.3	4.3	29.3
3600	4.17	0.00	528.1	0.88	642.9	262.4	2.21	6.1	51.3	87.9
3603	2.29	0.00	194.7	0.52	307.3	119.8	0.73	2.3	53.9	10.0
3609	1.94	0.00	14.1	0.06	8.9	8.5	0.43	0.1	1.3	3.5
3611	1.41	0.00	16.0	0.00	0.9	9.4	0.53	0.3	0.5	2.6
3612	2.17	0.00	15.7	0.25	0.8	9.8	0.19	0.3	0.4	1.2
3616.1	2.03	0.00	37.5	0.65	5.7	23.8	0.29	0.5	0.4	2.6
3616.2	3.10	0.00	40.6	0.23	9.6	25.3	0.25	0.4	2.6	0.8
3619.1	1.38	0.00	31.9	0.17	23.7	20.8	0.25	0.5	5.5	1.2
3619.2	2.01	0.00	32.3	0.16	2.9	20.8	0.21	0.4	0.8	1.4
3619.3	2.46	0.00	30.5	0.00	1.0	20.5	0.26	0.9	0.7	1.7
3619.4	2.34	0.00	30.2	0.19	12.3	21.5	0.21	1.7	0.8	5.8

Grey areas correspond to ice layers without visible inclusions (Ice-2). Only mean values are reported for large crystals where ionic distributions in ice lattice were also studied (see Section 4.1).

and may indicate that NaCl found in accretion ice does not come from air-transported marine salts.

In Fig. 4b, we have checked the relationship between SO_4^{2-} and the remaining significant cations, i.e. Mg^{2+} and Ca^{2+}. Although these two cations do not exhibit similar patterns, their sum is very well correlated with sulfate ($r = 0.996$) in accreted ice (stars), irrespective of the total ionic content. The slope of the regression line (0.84 ± 0.01) indicates that more than 80% of sulfate can be explained by various amounts of $CaSO_4$ and $MgSO_4$. This is not true in glacier ice (circles) where an excess of sulfate accounts for 70%

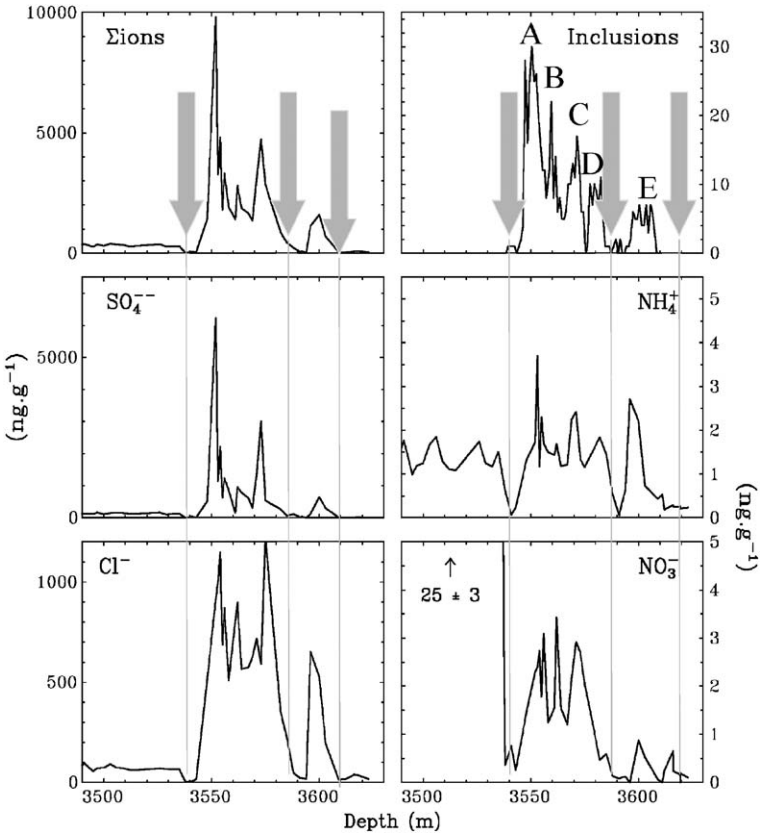

Fig. 3. Concentration trends within accreted ice. Concentrations, expressed in ng g^{-1}, are reported as a function of depth. Gray arrows and gray lines show accreted ice layers without visible inclusions (accreted ice-2, 3538–3553, 3588–3594, below 3608 m depth). $C1^-$,SO_4^{2-} and the ionic budget (Σions) are represented in the left part of the figure, NO_3^-, NH_4^- and the number of visible inclusions in the right part.

of the total sulfate mass. The proton concentration was not measured here but can be calculated in acidic or slightly acidic ice using the ionic balance ($H^+ = \Sigma$ anions (μEq l^{-1}) − Σ cations (μEq l^{-1})) [15,16]. In glacier ice where ionic balance is fairly constant and slightly positive (2.6 ± 0.6 μEq l^{-1}), excess sulfate is present as H_2SO_4. Analytical uncertainties (± 3–10 μEq l^{-1}) linked to very high ionic concentrations do not allow a direct comparison between the acidity of accretion ice-1 and the acidity of glacier ice. However, ionic balance drops to zero (0.0 ± 0.2 μEq l^{-1}) at 3538 m in the first layer of accretion ice-2, as expected in samples where salt contribution prevails. This transition from acidic to non-acidic ice takes place between 3535 and 3538 m and is in agreement with an ECM signal dropping to zero [6].

3.2.3. Ion distribution

An attempt to understand the role played by visible inclusions and grain boundaries on salts concentrations was made exploring detailed ionic distributions in the ice lattice. Accretion ice is made of large ice crystals of very high crystalline quality similar to that of single crystals carefully grown under laboratory conditions [17]. Five ice sections, 20 to 30 cm long made of very large crystals were cut lengthwise every 2.5 to 3 cm. Two were taken from accretion ice-1 (3553 and 3571 m) and three from accretion ice-2 (3541, 3591 and 3619 m). Typical ionic distributions are presented in Fig. 5. As already pointed out, concentrations are much higher in accretion ice-1. Only F^- exhibits no large change when passing from accretion ice-1 to accretion ice-2. Considering its very

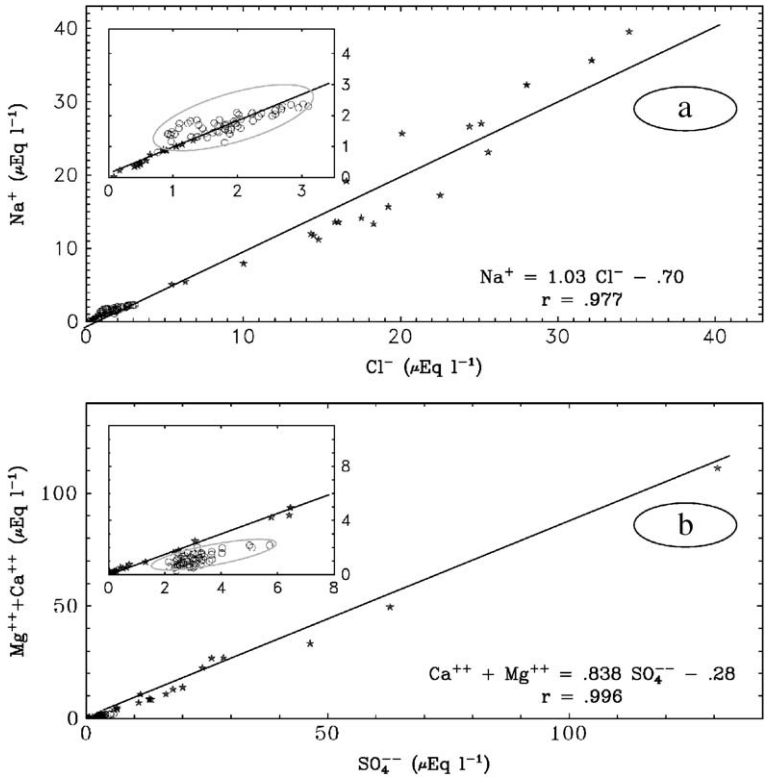

Fig. 4. Ionic associations in glacier ice (gray circles) and in accreted ice (black stars). Concentrations are expressed in μEq l^{-1}. a) Na^+ as a function of $C1^-$, b) (Mg^{2+} + Ca^{2+}) as a function of SO_4^{2-}.

high diffusion coefficient in ice [18], this ion is probably relocated after ice formation leading to apparently smoothed concentration gradients. Taking a pure diffusion coefficient value of 2×10^{-10} m s^{-2} for ice at -3 °C [19], it should take approximately 1500 years for fluoride to diffuse through a few meters of ice. This is consistent with a maximum age of 18,000 years for accretion ice at the Vostok site, based on an estimate of glacier ice velocity (~ 3 m $year^{-1}$ [7]) and flow trajectories across the lake. For a given ion, distribution patterns are very similar in accretion ice-1 and -2: Cl^-, Na^+, F^- and NO_3^- show very little change along individual crystals, while SO_4^{2-}, Ca^{2+}, Mg^{2+} and NH_4^+ show very strong variation. Cl^- and Na^+ are homogeneously distributed and in stoichiometric equilibrium, even when concentrations are very high (1000 ng g^{-1}). On the other hand, sulfate salts are distributed heterogeneously, even in the absence of visible inclusions, and high concentrations of pure $CaSO_4$ (3553 and 3541 m) or pure $MgSO_4$ (3553 m), are observed, separated by several cm of ice with lower concentrations. The distribution pattern does not seem to be significantly influenced by the presence of rare grain boundaries (denoted by arrows in Fig. 6). This was confirmed by the study of another ice section from 3553 m depth which was cut into two portions: the first contained one grain boundary and two large inclusions, while the second contained no grain boundary and only a few small inclusions [17]. Sulfate concentrations, mostly as $MgSO_4$, were higher in the first sample (4900 ng g^{-1}) than in the second (1000 ng g^{-1}), while Cl^- did not vary (1100 and 1200 ng g^{-1}, respectively). Crystalline features, dominated by $MgSO_4$, have been observed by energy dispersive X-ray microanalysis along the triple junctions of ice grains [20], but our results clearly demonstrate that grain boundaries do not gather all the impurities and that solid inclusions play an important role.

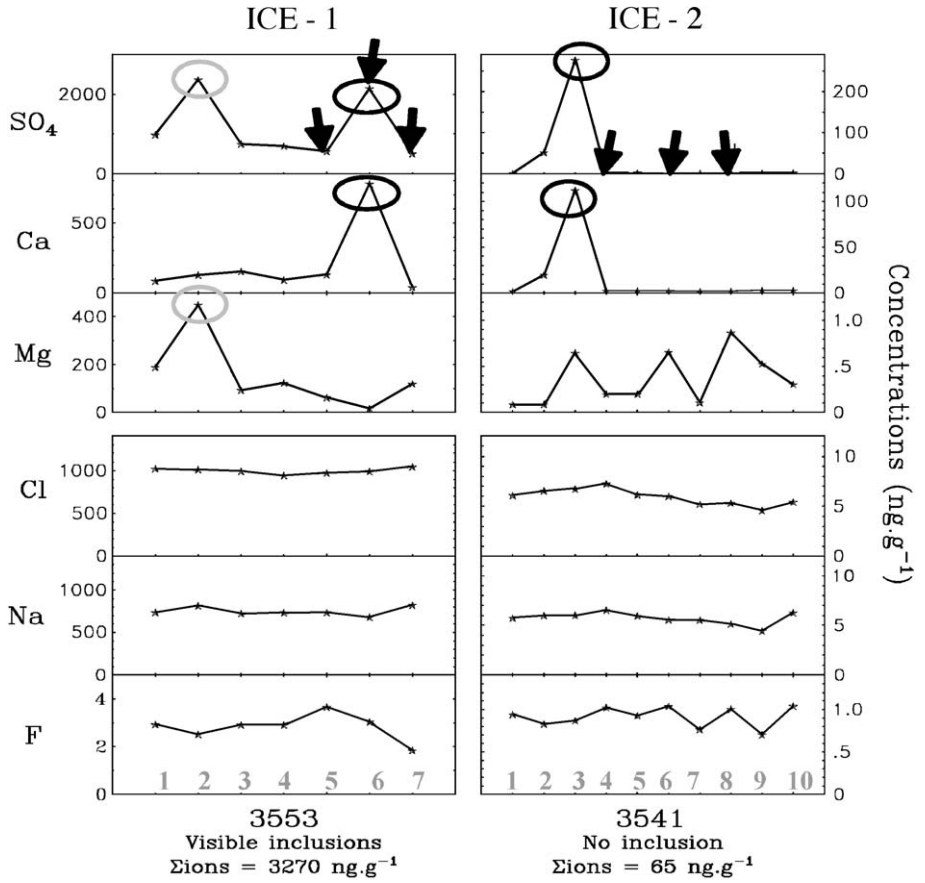

Fig. 5. Ionic distribution along two samples made of large crystals from 3553 m (left) and 3541 m (right) depth, respectively, cut lengthwise every 2.5 to 3 cm. F^-, Na^+, CL^- Mg^{2+}, Ca^{2+} and So_4^{2-} concentrations measured in consecutive sub-samples are expressed in ng g^{-1}. The horizontal axis uses arbitrary units and represents the successive ice sections taken along every crystal. Black arrows show samples where sub-structures, possibly grain boundaries, were observed. Black and gray circles show $CaSO_4$ and $MgSO_4$ occurrences, respectively. Σions is the ionic budget.

3.3. Sulfate isotopic composition

Sulfur and oxygen isotopes of sulfate have been recognized for decades as potential tools for source appointments [21] and are illustrative in the present case. Recent oxygen isotopic investigations of sulfate have revealed that sulfate formed in the atmosphere is mass-independently fractionated [22,23]. In most conventional processes (e.g. diffusion, kinetic reaction rate, phase change, etc.), the three stables oxygen isotopes of oxygen bearing species (^{16}O, ^{17}O, ^{18}O) are generally strictly correlated in a predictable manner. Using the conventional delta notation, mass-dependent compositions lie along the terrestrial mass dependent fractionation line (TFL) defined by the relation $\delta^{17}O \approx 0.52\ \delta^{18}O$ [23], while mass-independent compositions do not. The deviation from a mass-dependent fractionation relationship (i.e. mass-independent anomaly or oxygen-17 excess or deficiency) is represented by $\Delta^{17}O = \delta^{17}O - 0.512*\delta^{18}O$ (here 0.512 as determined from replicate analysis of samples and standards). Nonzero $\Delta^{17}O$ values have been observed only when reduced gaseous sulfur compounds are oxidized in the atmosphere [24], and can be used to determine the source origin of sulfate [25]. Atmospheric sulfate $\Delta^{17}O$ ranges between +1.3 ‰ to +4.8 ‰, with a mean of +3.2 ‰. Hundred thousand-year-old sulfate preserved in the Vostok ice core

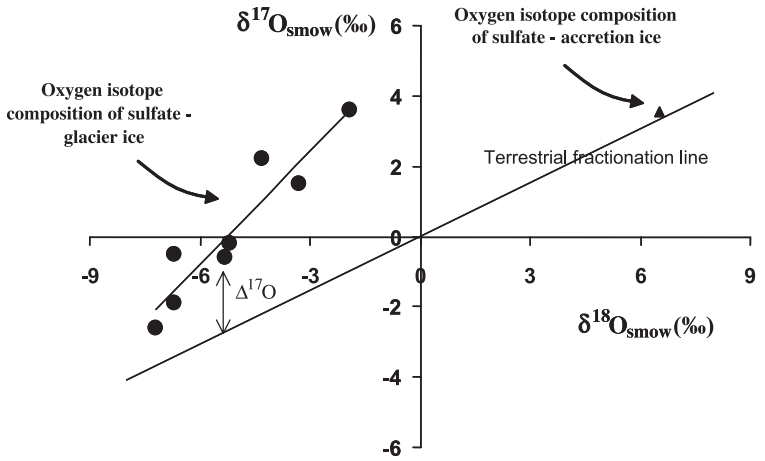

Fig. 6. Oxygen isotopic composition of sulfate in glacier ice (black dots) and in accretion ice (triangle, $\delta^{17}O_{smow} = 3.5‰$, and $\delta^{18}O_{smow} = 6.5‰$).

possesses such an oxygen isotopic anomaly [26]. This is expected for Antarctic central sites where, beside moderate and sporadic volcanic inputs, most of the sulfate present in glacier ice comes from the atmospheric oxidation of dimethylsulfide (DMS) emitted by marine biota [27,28]. Fig. 6 displays the value obtained for accreted ice along with results obtained by Alexander et al. in glacier ice [26]. From this figure, it is obvious that with a value of $+0.2‰$ ($\delta^{18}O = 6.5‰$, $\delta^{17}O = 3.5‰$), $\Delta^{17}O$ lies close to the TFL and differs significantly from what was found in upper glacier ice layers. These isotopic differences are underlined by $\delta^{18}O$ values.

4. Discussion

It can be conclude from Section 3 that glacier and accreted ice have different chemical fingerprints. This is puzzling and leads to the question of where the varying and sometimes very large amounts of NaCl and sulfate salts observed in accreted ice come from and how they are incorporated in the ice.

4.1. Incorporation of ionic impurities in accreted ice

The mechanism responsible for ice accretion is probably similar to that proposed for marine ice accreting under ice shelves [6]. It is likely initiated by the formation of frazil platelets in melted glacier water produced in the northern part of the lake and ascending along the North–South sloping glacier base. The frazil ice formation may require the presence of seed crystals [29]. The slush layer made of frazil crystals rising and accumulating under the glacier is consolidated by compaction, the slow freezing of host water and recrystallisation. Due to low supercooling levels, solute mainly present as salts may be segregated when superfusion breaks up, leading to heterogeneous distribution in ice and to chemical fractionation. Thus concentrations in seed crystals and in frazil ice can be expected to be significantly lower than in parent water. However, considering the rather stable ionic content of glacier ice, the composition of frazil ice is not expected to vary over a wide range, and changes in lake water composition or in parameters driving consolidation processes must be considered to explain the concentration–depth profiles observed in the sub-glacial ice.

Distribution coefficients close to 10^{-3} have been found for Cl^- solutions (HCl or NaCl) at atmospheric pressure, with freezing rates close to 1 cm h^{-1} [30,31]. Solute exclusion at the freezing front enhances ionic concentration in interstitial water close to the ice front, but this effect is partly counterbalanced by spontaneous convection. This results in a very slow increase of ion incorporation in the ice lattice with respect to the bulk host water composition. Selective

ionic exclusion was observed, smaller and negatively charged ions (Cl^- and F^-) remaining preferentially in the ice lattice. This observation is in agreement with the study of Moore et al. [32], referring to the ionic composition of ice of marine origin formed under the Ronne Ice Shelf (Antarctica). These authors have shown that large (SO_4^{2-}) or positively charged ions (Mg^{2+}, Na^+) were progressively excluded from the ice crystals and drained away by the brine, leaving Cl^- in the crystal, so that marine ice was depleted in SO_4^{2-}, Mg^{2+}, and Na^+ in comparison to the bulk sea water composition. Concentration changes with depth were smoothed and likely derived from changes in consolidation rate, with faster consolidation rates leading to lower fractionation effects.

Ice accretion in Lake Vostok takes place at a pressure of 33 MPa, and water is more compressible than ice, which could modify processes driving solute incorporation in the ice lattice and may lead to distribution coefficient values higher than expected from laboratory experiments. However, as accreted ice is made of frazil platelets and frozen host water in roughly similar proportions [6], we would expect a very low freezing rate for host water, i.e. in the range of 1 cm $year^{-1}$. For this reason, spontaneous diffusion close to the ice front should remain quite moderate. Gross [33] has observed that distribution coefficients decreased by several orders of magnitude as freezing rates decreased from $\sim$10 to $\sim$1 cm h^{-1} and freezing rates calculated for Vostok lake are more than two orders of magnitude lower than the latter value. Despite the possible pressure influence discussed above, this should lead to the quasi-total exclusion of most of the ions (except mainly Cl^- and F^-) from the accretion ice lattice, which is not supported by the scattered and sometimes very large amounts of salts found in accretion ice-1. In contrast, samples taken in the upper part of accretion ice-2 (3609–3619 m) depict much lower and more regular concentrations. Although they still contain very few and small inclusions, they are likely close in composition to ice formed right above the main lake, which allows us to tentatively estimate the lake salinity. For distribution coefficients of 10^{-3}–10^{-4}, NaCl concentration measured in these samples (25 to 50 ng g^{-1}) correspond to a water salinity of 0.05‰ to 0.3‰. This estimate is probably a minimum because freezing rates should be much lower than under ice shelves. In any case, at a pressure of 33 MPa, even a weak salinity must be taken into account when completing the picture of water circulation in Lake Vostok [4].

Despite an accretion rate lower by more than one order of magnitude than at the bottom of the Ronne Ice Shelf (45 cm $year^{-1}$ [34]), chloride concentrations in accretion ice-1 are only 10 times lower than in deeper levels of marine ice. This is surprising given the large contribution of glacier melt water to the lake water budget. Moreover, sulfate salt concentrations often significantly exceed NaCl concentrations, which is also quite unexpected. Finally, the complete vanishing of MSA with respect to sulfate is also very hard to explain in terms of selective exclusion at the freezing front. Both ionic concentrations and distribution along individual crystals (see Section 3.3) suggest that impurities were not only incorporated by mechanisms similar to those commonly observed under ice shelves, i.e. frazil ice consolidated by freezing host water, but also require additional mechanisms related to environmental conditions prevailing in the bay where ice accretion takes place. Some of the ions (SO_4^{2-}, Ca^{2+}, Mg^{2+} and NH_4^+) were probably present in the form of insoluble materials suspended in lake water, while the others (Cl^-, Na^+, F^- and NO_3^-) remained in solution within slush until the end of the consolidation process. Fine particles of $MgSO_4$ or/and $CaSO_4$ may have been carried upward by turbulent convection of NaCl rich water or by ascending frazil platelets and incorporated into the frazil slush. They are located in scattered solid inclusions of various sizes, present even in clear ice. In contrast, NaCl (like F^- and NO_3^-) appears to be included in the ice lattice. Considering that a very low freezing rate should lead to Na^+ preferential exclusion at the freezing front [31], NaCl was initially more likely present in very fine frozen brine pockets, homogeneously distributed at the mm scale. During crystal growth, which takes place after initial freezing, when accretion ice is transported across the lake at a temperature close to the melting point [17], ice-soluble ionic species like Cl^-, Na^+, F^- or NO_3^- should become more efficiently distributed throughout ice lattice, while the other ions or very fine sulfate salt particles, which are not in equilibrium with the ice lattice, should be excluded and gathered in inclusions of increasing sizes. Our data are con-

sistent with a solubility limit of 300 μM for Cl^- in ice lattice [32].

4.2. Possible origin of salts

The lake was probably formed several millions years ago. Magnetic, gravity, and subglacial topography data combined with gravity modeling support the hypothesis that the Lake Vostok basin is a tectonic feature of a large continental collision zone. The lake was formed on a pre-existing sedimentary basin, infilling a passive over-thrust continental margin, and collapsed after a minor extensional reactivation of the basal thrust fault [36]. The continental margin of the Vostok collision zone and its over-thrusting are expected to be Proterozoic in age [36]. The over-thrusting unit should be close in composition to continental shield regions south of Africa and Australia [37,38], i.e. metamorphic rocks. Sediments may be a mixture of remnant margin and foreland sedimentary sequences [36]. Taking this scenario into account, three main processes may be proposed to explain the impurity content and distribution found in accretion ice-1.

4.2.1. Pre-concentration of glacier meltwater

Increasing amounts of all ionic species initially present in glacier ice may enter lake water via a melting (glacier water input)–refreezing (clean ice export) process. Residence times ranging between 4500 and 125,000 years have been estimated for lake water [1,7,35]. If the lake was formed at the onset of Antarctic glaciation ~20 Ma BP, a maximum pre-concentration factor (with respect to glacier composition) of 4400 can be calculated, corresponding to the lower estimate of residence time (4500 years). This gives an upper limit of 0.3‰, 0.6‰, 0.04‰ and 0.05‰ for Cl^-, SO_4^{2-}, Mg^{2+}, and Ca^{2+} concentrations, respectively. These values are lower than those measured in sea water (20–35‰, 3‰, 2‰ and 0.6‰ for Cl^-, SO_4^{2-}, Mg^{2+}, and Ca^{2+}, respectively) and thus well below saturation concentrations for NaCl, $CaCO_3$, $CaSO_4$ or $MgSO_4$ observed in evaporating saline lakes, demonstrating that enrichment via a melting–refreezing process cannot have lead to the presence of fine magnesium and calcium sulfate particles in the lake water. Moreover, for distribution coefficient values of 10^{-3}–10^{-4}, NaCl concentrations as high as 2 μg g^{-1} observed in accreted ice imply a water salinity of 2‰ to 20‰. Such values cannot be reached through glacier melt-water preconcentration and require an additional source of NaCl. The minor role played by glacier melt-water recycling in lake water composition is confirmed by the oxygen isotope composition of sulfate. Indeed, the absence of strong oxygen anomaly in sulfate from one accretion ice sample (see Section 3.4) supports the idea that this ion has mainly a non-atmospheric origin in accreted ice. Considering a mixture of atmospheric and non-atmospheric sulfate contributions, a maximum of 6% may be attributed to glacier water recycling.

4.2.2. Bedrock weathering by sub-glacial or lake water

Glacial abrasion is not expected to significantly contribute to accretion ice content. Indeed, as observed from 3450 to 3538 m depth [39], large particles produced at the bed are incorporated to flowing ice before the glacier reaches the lake. Part of them may be lost to lake water by subglacial melting in the southern part of the lake, but they should rapidly settle to deeper water column. On the other hand, chemical weathering of bedrock minerals may have supplied lake water with some metal cations or dissolved carbonate and silica species. The most important mechanism by which rock minerals are weathered is acid hydrolysis, which requires the presence of melt-water and a source of H^+ ions. Sub-glacial melting occurs mostly at the glacier–lake interface, but a maximum melting rate of 1 mm $year^{-1}$ may be expected at the glacier bedrock interface for a geothermal flux value close to 50 mW m^{-2} [40]. Chemical weathering may also occur at the lake–bedrock interface. Since the system is closed with respect to atmospheric CO_2, the H^+ source may be from glacier water itself or from the weathering of sulfide (commonly pyrite) [41]. Even if all H_2SO_4 present in slightly acidic glacier water had reacted to form $MgSO_4$ or $CaSO_4$, these salts would have remained far below saturation concentrations close to the bedrock and in lake water. Pyrite hydrolysis produces soluble sulfate and insoluble particles of Fe_2O_3 or FeOOH. Additional Fe measurements were made by Inducted Coupled Plasma Optical Emission Spectroscopy (ICP OES) in three samples from depths of

3554, 3556 and 3562 m where high SO_4^{2-} concentrations (2207, 1236, 952 ng g^{-1}, respectively) were measured. Low Fe concentrations (22, 23 and 26 ng g^{-1}, respectively) associated with low insoluble microparticle content (~ 100 ng g^{-1}) were found. As previously discussed, sulfate is probably present as fine particles in solid inclusions. It may have precipitated at the glacier–bedrock interface if the water became saturated, but this is not expected given the very low flushing rate [40] and equilibrium consideration [41], or in the lake through pre-concentration processes. Even if initially produced in the melting area and transported in the slowly ascending water plume, iron or sulfate particles should progressively settle to deeper layers before reaching the accretion zone. Although this is not a decisive argument, the very large difference between Fe and SO_4^{2-} concentrations suggests that bedrock hydrolysis does not play a prominent role in lake water and accretion ice composition. Another argument may be that Ca^{2+} is the dominant cation in most sub-glacial melt-waters while Cl^- concentrations are generally very low [40], which is quite different from the conditions in the accretion ice, where high NaCl concentrations are observed. Based on its oxygen isotope composition, it has been demonstrated that sulfate in accretion ice has mostly a non-atmospheric origin. A $\delta^{34}S$ value of +9.2‰ (CDT) was observed for the sulfur isotope composition. Many sources of non-atmospheric sulfate, mineral or organic, have narrow sulfur isotopic signatures, making it difficult to determine the origin of sulfate in accreted ice. However, the association of very large NaCl, $MgSO_4$, and $CaSO_4$ concentrations support the possibility that the sulfur isotopic composition comes from a mixture of sea salt evaporites ($\delta^{34}S \sim +21$‰) and lithospheric sources ($\delta^{34}S \sim 0$‰) [29].

4.2.3. Pre-existing sedimentary basin

Large and varying amounts of evaporitic-like material (brine water or solid salt particles) may enter accreted ice by the sporadic injection of NaCl and sulfate salts from a reservoir not directly or permanently connected with the lake water.

The bedrock under Lake Vostok and in the adjacent large Aurora basin lies below present sea level (−1000 m). This is only partly explained by the isostatic depression due to the ice load, which is estimated to account for ca. 800 m [42]. The deepest valleys may likely have been flooded by the sea, particularly during the large cretaceous transgression [37,38], leading to evaporite formation when the seawater evaporated, as observed for many graben structures (e.g. the Rhine valley, between the German Black Forest and the French Vosges regions, where many salt mines are found). Once formed, evaporite strata were buried by subsequent sediment sequences. The presence of a major border fault system on the eastern shoreline of the lake raises the possibility of fluid convection by the transport of ground water (slightly warmer than lake water) along faults cropping out into the lake [40]. Such a mechanism may make possible the transfer of material from an evaporite-rich deeper reservoir into the lake water. Moreover, seismo-tectonic activity, as currently observed in the lake vicinity [40], could activate from time to time or boost exchange processes between the two reservoirs.

If dissolved halite and fine solid debris are transported upward by convection processes, their incorporation in accretion ice requires that slush consolidation is more rapid than expected. This could occur in the shallow bay upstream from Vostok site (see Fig. 1), which is partly closed by a ridge against which the glacier is moving and pushing, thereby compacting the loose frazil ice. Mechanically strained compaction of the slush could lead to more rapid densification and transformation into accreted ice. This process is in agreement with the much cleaner ice accreting above the main lake.

5. Conclusion

A detailed study of the ionic content of the deepest part of the Vostok core, combined with specific investigations of selected samples, shows that accretion ice is significantly different in composition from glacier ice. Large and varying concentrations of salts, dominated by halite and calcium or magnesium sulfate, are observed in ice accreted ice above the subglacial lake. Some of these salts are homogeneously distributed throughout the ice lattice (halite, fluoride and nitrate), while the remaining (sulfate and ammonium salts) seem to be preferentially located in scattered solid inclusions or, to a lesser extent, at grain

boundaries. Chemical considerations supported by additional isotopic and Fe measurements strongly suggest that these salts originate from deeper sedimentary strata, close to evaporites in composition. Considering the possible geological history of Lake Vostok and the bottom topography, a scenario is proposed that explains both the composition and the distribution of impurities in accreted ice. Inclusion-rich and salty ice likely forms in a shallow bay upstream from Vostok on the northeastern side of the lake, while ice without visible inclusion, containing very few impurities, forms when the glacier passes over the deep main lake.

Acknowledgements

Vostok ice cores were recovered by a joint Russia, France and USA program. We thank the Russian Antarctic Expeditions, the Institut Polaire Paul Emile Victor and the Division of Polar Programs (NSF) for logistic support. We are grateful to the drilling team (St. Petersburg Mining Institute) for field work, and R. Souchez acknowledges the support of the Belgian Antarctic Program (Science Policy Office). We wish to thank Paul Duval for helpful discussion as well as Becky Alexander and Justin McCabe for their help in processing the sulfate sample for isotope analysis and Martin Shock for DOC measurements. ***[EB]***

References

[1] A.P. Kapista, J.K., Ridley, G. de Q. Robin, M.J. Siegert, I.A. Zotikov, A large deep freshwater lake beneath the ice of central East Antarctica, Nature 381 (1996) 684–686.

[2] J.A. Dowdeswell, M.J. Siegert, The dimension and topography setting of Antarctic subglacial lakes and implications for large-scale water storage beneath continental ice sheets, GSA Bull. 1112 (1999) 254–263.

[3] J. Jouzel, J.-R. Petit, R. Souchez, N.I. Barkov, V.Ya. Lipenkov, D. Raynaud, M. Stievenard, N.I. Vassiliev, V. Verbeke, F. Vimeux, More than 200 meters of lake ice above subglacial Lake Vostok, Antarctica, Science 286 (1999) 2138–2141.

[4] M.J. Siegert, Antarctic subglacial lakes, Earth-Sci. Rev. 50 (2000) 29–50.

[5] M.J. Siegert, M. Ellis-Evans, M. Tranter, C. Mayer, J.-R. Petit, A. Salamatin, J. Priscu, Physical, chemical and biological processes in Lake Vostok and other Antarctic subglacial lakes, Nature 414 (2001) 603–609.

[6] R. Souchez, J.-R. Petit, J.-L. Tison, J. Jouzel, V. Verbeke, Ice formation in subglacial Lake Vostok, Central Antarctica, Earth Planet. Sci. Lett. 181 (2000) 529–538.

[7] R.E. Bell, M. Studinger, A.A. Tikku, G.K.C. Clarke, M.M. Gutner, C. Meertens, Origin of Lake Vostok water frozen to the base of the East Antarctic ice sheet, Nature 416 (2002) 307–310.

[8] C. Saigne, S. Kirchner, M. Legrand, Ion-chromatographic measurements of ammonium, fluoride, acetate, formate and methanesulphonate ions at very low levels in Antarctic ice, Anal. Chim. Acta 203 (1987) 11–21.

[9] J. Savarino, B. Alexander, V. Darmohusodo, M.H. Thiemens, Sulfur and oxygen isotope analysis of sulfate at micromole levels using a pyrolysis technique in a continuous flow system, Anal. Chem. 73 (2001) 4457–4462.

[10] J. Farquhar, T.L. Jackson, M. Thiemens, A S 33 enrichment in ureilite meteorites: evidence for a nebular sulfur component, Geochim. Cosmochim. Acta 64 (2000) 1819–1825.

[11] X. Gao, M.H. Thiemens, Systematic study of sulfur isotopic composition in iron meteorites and the occurrence of excess 33S and 36S, Geochim. Cosmochim. Acta 55 (1991) 2671–2679.

[12] X. Gao, M.H. Thiemens, Isotopic composition and concentration of sulfur in carbonaceous chondrites, Geochim. Cosmochim. Acta 57 (1993) 3159–3169.

[13] R. Souchez, J.-R. Petit, J. Jouzel, M. De Angelis, N. Barkov, M. Stiévenard, F. Vimeux, S. Sleewaegen, R. Lorrain, Highly deformed basal ice in the Vostok ice core, Antarctica, Geophys. Res. Lett. 29 (2002) 40-1-4.

[14] D.M. Karl, D.F. Bird, K. Björkman, T. Houlihan, R. Shackelford, L. Tupas, Microorganisms in the accreted ice of Lake Vostok, Antarctica, Science 286 (1999) 2144–2147.

[15] M. Legrand, J.-R. Petit, Y.S. Korotkevich, D.C. Conductivity of antarctic ice in relation to its chemistry, J. Phys., Colloq. C1 48 (Suppl. 3) (1987) C1-605–C1-611.

[16] F. Maupetit, R.J. Delmas, Snow chemistry of high altitude glaciers in French Alps, Tellus 46B (1994) 304–324.

[17] M. Montagnat, P. Duval, P. Bastie, B. Hamelin, O. Brissaud, M. de Angelis, J.-R. Petit, V.Ya. Lipenkov, High crystalline quality of large single crystals of subglacial ice above Lake Vostok (Antarctica) revealed by hard X-ray diffraction, C. R. Acad. Sci. Paris, Earth Planet. Sci. 333 (2001) 419–425.

[18] P.V. Hobbs, Ice Physics, Clarendon Press, Oxford, 1974, 837 pp.

[19] M. Kopp, D.E. Barnach, I.J. Lowe, Measurements by NMR of the diffusio of HF in ice, J. Chem. Phys. 43 (1965) 2965–2971.

[20] D. Cullen, I. Baker, Observation of sulfate crystallites in Vostok accretion ice, Mater. Charact. 48 (2002) 263–269.

[21] H.R. Krouse, V.A. Grinenko, Stable isotopes: natural and anthropogenic sulfur in the environment, Published on behalf of the Scientific Committee on Problems of the Environment (SCOPE) of the International Council of Scientific Unions (ICSU) in collaboration with the United Nations Environment Program by Wiley and Sons, 1991.

[22] C.C.W. Lee, M.H. Thiemens, δO^{17} and δO^{18} measurements of atmospheric sulfate from coastal and high alpine region: a

mass independent isotopic anomaly, J. Geophys. Res. 106 (2001) 17359–17374.
[23] C.W. Lee, J. Savarino, M.H. Thiemens, Mass independent isotopic composition of atmospheric sulfate: origin and implications for the present and past atmosphere of Earth and Mars, Geophys. Res. Lett. 28 (2001) 1783–1786.
[24] M.H. Thiemens, Mass-independent isotope effects in planetary atmospheres and the solar system, Science 283 (1999) 341–345.
[25] H. Bao, D.A. Campbell, J.G. Bockheim, M.H. Thiemens, Origin of sulfate in Antarctic dry valleys soils as deduced from anomalous 17O compositions, Nature 407 (2000) 499–502.
[26] B. Alexander, J. Savarino, N.I. Barkov, R.J. Delmas, M.H. Thiemens, Climate driven changes in the oxidation pathways of atmospheric sulfur, Geophys. Res. Lett. 29 (14) (2002) 301–304.
[27] M. Legrand, Sulphur-derived species in polar ice: a review, in: R.J. Delmas (Ed.), Ice Core Studies of Global Biogeochemical Cycles, NATO ASI Series I Global Environmental Change, vol. 30, Springer-Verlag, Berlin, Heidelberg, 1995, pp. 91–120.
[28] M. Legrand, D. Wagenbach, Impact of the Cerro Hudson and Pinatubo volcanic eruptions on the Antarctic air and snow chemistry, J. Geophys. Res. 104 (1999) 1581–1596.
[29] A. Jenkins, A. Bombosch, Modeling the effects of frazil ice crystals on the dynamics and thermodynamics of ice shelf water plumes, J. Geophys. Res. 100 (1995) 6967–6981.
[30] G.W. Gross, C.H. Wu, L. Bryant, C. McKee, Concentration dependent solute redistribution at the ice/water phase boundary: II. Experimental investigation, J. Chem. Phys. 62 (1975) 3085–3092.
[31] G.W. Gross, P.M. Wong, K. Humes, Concentration dependent solute redistribution at the ice/water phase boundary: III. Spontaneous convection of chloride solutions[a)], J. Chem. Phys. 67 (1977) 5264–5273.
[32] J.C. Moore, A.P. Reid, J. Kipfstuhl, Microstructure and electrical properties of marine ice and its relationship to meteoric ice and sea ice, J. Geophys. Res. 99 (1994) 5171–5180.
[33] G.W. Gross, Ion distribution and phase boundary potentials during the freezing of very dilute ionic solutions at uniform rates, J. Colloid Interface Sci. 25 (1967) 270–279.
[34] H. Engelhardt, J. Determann, Borehole evidence for a thick layer of basal ice in the central Ronne Ice Shelf, Nature 327 (1987) 318–319.
[35] P. Jean-Baptiste, J.-R. Petit, V.Ya. Lipenkov, D. Raynaud, N.I. Barkov, Constraints on hydrothermal processes and water exchange in Lake Vostok from Helium isotopes, Nature 411 (2001) 460–462.
[36] M. Studinger, G.D. Karner, R.E. Bell, V. Levin, C.A. Raymond, A.A. Tikku, Geophysical models for a tectonic framework of the Lake Vostok region, East Antarctica, Earth Planet. Sci. Lett. 216 (2003) 663–677.
[37] A.M. Ziegler, C.R. Scotese, W.S. McKerrow, M.E. Johnson, R.K. Bambach, Paleozoic paleogeography, Annu. Rev. Earth Planet. Sci. 7 (1979) 473–502.
[38] C.R. Scotese, R.K. Bambach, C. Barton, R. Van de Voo, A.M. Ziegler, Paleozoic base maps, J. Geol. 87 (1979) 217–277.
[39] J.C. Simões, J.-R. Petit, R. Souchez, V.Ya. Lipenkov, M. De Angelis, L. Liu, J. Jouzel, P. Duval, Evidence of glacial flour in the deepest 89 m of the Vostok ice core, Ann. Glaciol. 35 (2002) 340–346.
[40] M. Studinger, R.E. Bell, G.D. Karner, A.A. Tikku, J.W. Holt, D.L. Morse, T.G. Richter, S.D. Kempf, M.E. Peters, D.D. Blankenship, R.E. Sweeney, V.L. Rystrom, Ice cover, landscape setting and geological framework of Lake Vostok, east Antarctica, Earth Planet. Sci. Lett. 6463 (2002) 1–16.
[41] R. Raiswell, A.G. Thomas, Solute acquisition in glacial melt waters: I. Fjallsjökull (South-East Iceland): bulk melt waters with closed-system characteristics, J. Glaciol. 30 (1984) 35–43.
[42] D.J. Drewry, Antarctica: Glaciological and Geophysical Folio, Scott Polar research Institute, Cambridge, 1983.